

PHILOSOPHICAL  
TRANSACTIONS A[rsta.royalsocietypublishing.org](http://rsta.royalsocietypublishing.org)

Research



Article submitted to journal

**Subject Areas:**

xxxxx, xxxxx, xxxxx

**Keywords:**

xxxx, xxxx, xxxxx

**Author for correspondence:**

Insert corresponding author name

e-mail: [xxx@xxxx.xx.xx](mailto:xxx@xxxx.xx.xx)GaN micro-LED structured  
light sources for multi-modal  
optical wireless  
communications systemsA. D. Griffiths<sup>1</sup>, J. Herrnsdorf<sup>1</sup>,  
J. J. D. McKendry<sup>1</sup>, M. J. Strain<sup>1</sup> and  
M. D. Dawson<sup>1</sup><sup>1</sup>Institute of Photonics, Department of Physics,  
University of Strathclyde, Glasgow, G1 1RD

Gallium nitride based light-emitting diodes (LEDs) have revolutionised the lighting industry with their efficient generation of blue and green light. While broad-area (square mm) devices have become the dominant LED lighting technology, fabricating LEDs into micro-scale pixels (micro-LEDs) yields further advantages for optical wireless communications (OWC), and for the development of smart-lighting applications such as tracking and imaging. The smaller active areas of micro-LEDs result in high current density operation, providing high modulation bandwidths and increased optical power density. Fabricating micro-LEDs in array formats allows device layouts to be tailored for target applications and provides additional degrees of freedom for OWC systems. Temporal and spatial control is crucial to utilise the full potential of these micro-scale sources, and is achieved by bonding arrays to pitch-matched complementary metal-oxide-semiconductor (CMOS) control electronics. These compact, integrated chips operate as digital-to-light converters, providing optical signals from digital inputs. Applying the devices as projection systems allows structured light patterns to be used for tracking and self-location, while simultaneously providing space-division multiple access communication links. The high speed nature of micro-LED array devices, combined with spatial and temporal control, allows many modes of operation for OWC providing complex functionality with chip-scale devices.

## 1. Introduction

The wireless transmission of data is ubiquitous in the modern world, with both the number of devices and volume of data transfer ever increasing to support a wirelessly connected internet of things. The dominant technology for wireless communications is currently radio frequency (RF), though it is expected that RF capacity will be unable to keep pace with the current increases in demand [1]. It is therefore unlikely that future wireless communication will be dominated by a single technology. Optical wireless communications (OWC) involves data transmission using optical frequencies (ultraviolet, visible and infrared), and is an attractive, complementary approach which may ease the capacity strain on RF communications. Moving to the optical spectrum has a number of benefits, including: wide unlicensed bandwidth, no interference with RF signals, and spatial reuse and security through signal confinement [2]. In the more specific case of light-emitting diode (LED) transmitters, advantages also include energy efficiency, low cost, size, weight and power, and the potential for integration into current solid state lighting (SSL) for “Li-Fi” (Light-Fidelity) style systems [3].

The source technologies that underpin visible light OWC include Gallium Nitride (GaN) LEDs [4], III-Phosphide LEDs [5], organic/colloidal quantum dot/perovskite LEDs [6–8], and visible light semiconductor lasers [9]. Among these, GaN LEDs have seen a high level of research activity because they offer a combination of robustness, high performance, technological simplicity, maturity and versatile device formats with routes to scalable manufacture. A format that offers a particularly rich array of opportunities is microscale GaN LEDs with a size of less than 100  $\mu\text{m}$ , referred to as “micro-LEDs”. Individual micro-LEDs have intriguing properties on their own, as their dimensions enable unique operating conditions such as high current densities. This, in turn, allows high modulation bandwidths of 100s of MHz, making these devices attractive for OWC (see Section 2). Notably, micro-LEDs are typically operated as arrays, adding a spatial degree of freedom to the LED modulation and significantly extending their applications beyond the capabilities of conventional broad area LEDs. Importantly, micro-LEDs are also emerging as a new format of high brightness and fast response display technology, therefore offering routes to convergence between lighting, display and communication technologies.

This article will discuss the particular characteristics of micro-LEDs, the challenges in interfacing and driving high density arrays, and the application areas opened up by the devices that have been developed. In Section 2, the characteristics of micro-LED pixels are discussed, while Section 3 covers driving and interfacing methods for high density micro-LED arrays. In Section 4, recent work on OWC with micro-LED sources is presented. Section 5 discusses multi-functional OWC enabled by the structured light projection from micro-LED devices. Finally, Section 6 draws some conclusions and provides an outlook on future work.

## 2. Characteristics of micro-LEDs for OWC

LEDs are increasingly widespread devices used in a broad range of applications, currently revolutionising indoor and street lighting [5], and set to play an increasingly important role in display technology. The III-V compound semiconductor alloys can provide devices with emission wavelengths across the full visible spectrum, extending into the ultraviolet and infrared. With efficient blue-emitting devices available from GaN based materials, white light can be generated with the addition of a suitable phosphorescent/fluorescent layer, or in combination with other LED sources emitting at longer wavelengths, enabling solid-state lighting [10]. The advantages of LED-based lighting over other previous lighting technologies, particularly in efficiency and operational lifetime, are now well known. However, the semiconductor nature of LEDs offers ready interfacing to advanced electronics and allows applications to be investigated far beyond simple illumination. A prominent example is Li-Fi technology, which can use either broad area or micro-LEDs, though the micro-LED format enables a range of capabilities that are largely inaccessible to broad area LEDs.

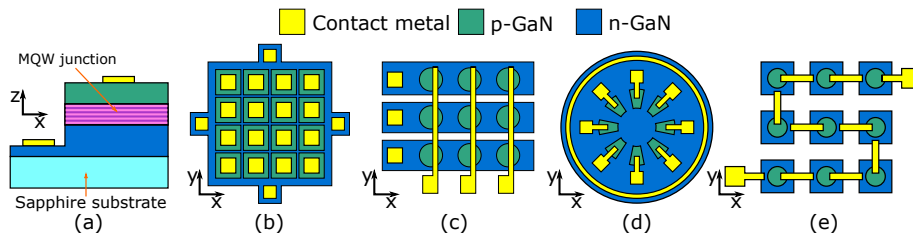


**Figure 1.** Schematics of micro-LED structure and array formats (not to scale): (a) Side view of a pixel's vertical structure and plan views of (b) active-matrix array, (c) passive-matrix array, (d) low density array, (e) series connected array.

Micro-pixelated arrays of inorganic LEDs can also be used as passive or active matrix displays, which offer high brightness compared to existing liquid crystal or organic LED technologies [11, 12], can be readily combined with nanocrystal colour converters for a large colour gamut [13], and are likely to play a significant role in emerging display technologies. For such an application, devices will need to provide around 100 fps refresh rates over a great number of pixels. However, each pixel in an array has a fast modulation response, and while backplane electronics with matching response will be difficult to achieve for high pixel numbers, smaller scale arrays are attractive for OWC using the schemes discussed in sections 4 and 5. The exact properties of the micro-LEDs depend on the device format, electronic interfacing, and driving conditions.

### (a) Fabrication and format

Inorganic LEDs are fabricated from wafers with epitaxially deposited semiconductor films, which include p-doped and n-doped layers, a multi-quantum-well junction region, and possibly other functional layers such as an electron blocking layer [14]. GaN based epitaxial structures are commonly grown on sapphire substrates, though silicon and bulk GaN wafers are also in use [15]. The use of transparent substrates in particular, such as sapphire, enables a flip-chip device format which is crucially exploited in flip-chip active matrix devices [16,17].

Individual LED pixels are fabricated by etching mesas into the epitaxial structure of the wafer, isolating an area of the active region and allowing access to both the n-doped and p-doped regions for electrical contact. Mesas are defined with photolithographic patterning followed by inductively-coupled plasma (ICP) etching and contacted through deposition of metal tracks and pads, resulting in the structure shown in the schematic cross section in Fig. 1(a). Various pixel arrangements can be defined through design of the photolithography masks, allowing micro-LED arrays to be tailored for specific applications. High-density active- or passive-matrix arrays (Fig. 1(b) and (c), respectively) were originally designed for display applications, but are now also used for structured illumination, digital-to-light conversion and other related techniques. Low-density arrays of individually connected micro-LEDs (Fig. 1(d)) have proven useful for high data rate multiple-input multiple output (MIMO) OWC. Micro-LED arrays without pixel-addressing capability, e.g. through series connection (Fig. 1(e)), have also shown attractive properties [18]. Sections 4 and 5 highlight how these device formats relate to particular applications.

### (b) Active-matrix arrays

Early generations of LED displays such as alphanumeric indicators and dot-matrix displays were fabricated in a passive-matrix format, requiring continuous line-scanning for the display of arbitrary patterns. While impressive demonstrations are still being made with such devices today, including e.g. a 1000 fps single-pixel camera [19], there are clear scalability issues, with traditional displays starting to experience flicker-issues when going beyond 0.01 Megapixels [20]. Addressing pixels in an array with direct, individual contacts, with separate electronic drivers, is

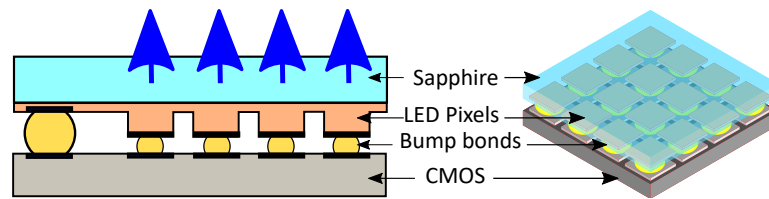


**Figure 2.** Schematic of a micro-LED array bump-bonded to a CMOS control chip. The flip-chip format of the array means light is extracted through the sapphire substrate, which is polished.

even more limiting as the space requirements of the metal tracks make it difficult to create arrays larger than  $10 \times 10$  [21].

Therefore, an important advance was made by the introduction of active-matrix arrays, where each micro-LED pixel has its own driver circuit, which in turn is controlled through a digital electronic bus. One approach is to develop monolithic devices, with both LED pixels and transistors fabricated in a single GaN-based epitaxial structure [22]. However, this approach has several challenges including the complexity of the required epitaxial structure and difficulties in obtaining a high area fill factor. Instead, digital drivers can be readily implemented in complementary metal-oxide-semiconductor (CMOS) control electronics, in an arrayed format matching that of a micro-LED array. Vertically stacking the micro-LED array on top of the CMOS control array, using flip-chip bump bonding, provides a mm-scale chip with digital control of optical emission. Each LED pixel has an individual set of drive electronics and light is extracted through the optically transparent sapphire substrate as shown in Fig. 2. Complex digital drive electronics can be implemented, allowing additional functionality for an active-matrix micro-LED system such as pulse width modulation (PWM), memory buffers for image display, and short pulse operation [16,23]. Additionally, more complex, analogue modulation can be performed using an integrated driving approach by developing CMOS electronics with a current-steering digital-to-analogue converter (DAC) to drive the micro-LED pixels [24]. Besides flip-chip bonding, integration of GaN micro-LEDs with CMOS drivers can also be achieved through transfer printing individual LED pixels from the growth substrate onto the CMOS chip [25]. This approach produces devices with high uniformity and low optical cross-talk, though the process has a low level of maturity.

### (c) Modulation characteristics

LED performance under DC operation is characterised by the relationships between bias voltage, current draw and output optical power. Fig. 3 (a) shows the current in a micro-LED pixel as a function of bias voltage. An immediately clear feature is the very high current density operation in micro-LEDs, in excess of  $1 \text{ kA cm}^{-2}$ , compared to typical broad area devices operating around  $100 \text{ A cm}^{-2}$ . Fig. 3(b) shows the output power density, dependent on the current density, displaying the high brightness performance of micro-LED pixels. The non-linear relationships between current, voltage and output optical power shown have important consequences in the modulated driving of micro-LEDs, and this is discussed in detail in section 3.

To transmit optical wireless communication signals the micro-LED transmitter must emit a modulated optical signal. Output intensity modulation is achieved by applying a modulated electrical signal in combination with DC bias conditions, but there will ultimately be a limit to how rapidly a device can respond to the input signal. An important parameter of a device is therefore the optical modulation bandwidth that can be achieved, defined as the frequency at which the power of the optical signal is reduced to half, or -3 dB. On an electrical frequency response curve from a photodetector, this corresponds to the -6 dB point, as received electrical power is proportional to the square of the photocurrent generated by incident optical power. Fig. 3(c) shows the modulation bandwidth of a range of micro-LED pixels versus increasing

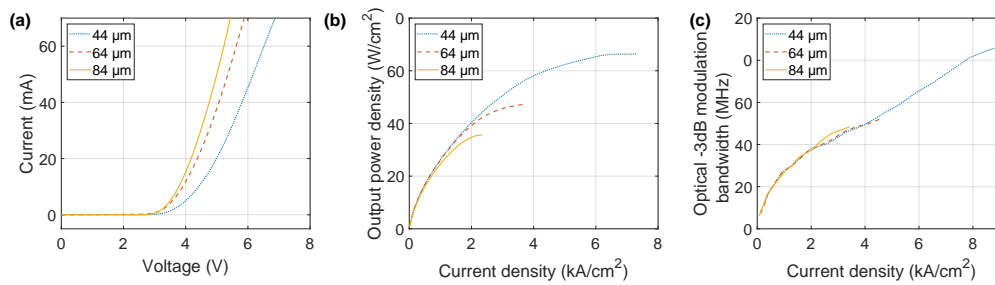


**Figure 3.** Example (a) I-V, (b) L-I and (c) modulation bandwidth characteristics of circular, blue (450 nm) micro-LED pixels with varying diameters [26]. Output power density was measured externally at the sapphire face.

current density. This bandwidth was measured by applying a DC-offset small-signal sinusoidal signal. Increasing the DC bias, and therefore injected current density, increases the modulation bandwidth.

For a broad area LED, the modulation bandwidth is typically limited by the RC (resistance - capacitance) constant of the device, which is on the order of nanoseconds for devices with an area on the order of  $1 \text{ mm}^2$ . In contrast, for a  $100 \times 100 \text{ μm}^2$  micro-LED, the RC constant is estimated to be on the order of 200 ps [27], and thus for such small devices, other parameters limit the bandwidth. When comparing the bandwidths of micro-LEDs with different sizes (Fig. 3(c)), we observe the same bandwidth at a given current density regardless of the micro-LED area. This indicates that the bandwidth is determined by the differential carrier lifetime in the active region [26]. This can be understood by the current-density dependence of carrier lifetimes in semiconductors, which are often approximated by the popular ABC model [28]. An increase in current density results in an increase in the carrier density within the active region, which in turn results in increased radiative and higher order (Auger) recombination rates, directly improving modulation bandwidth [29]. It should be noted that the device physics of GaN LEDs are notoriously complicated and both RC constant estimates and ABC model analysis need to be interpreted with care [27,30]. However, they are useful to understand the dominating factors affecting the modulation characteristics.

### 3. Driving modes and electronic interfacing

#### (a) Individual pixel driving

Intensity modulation of an LED transmitter is typically performed by applying an AC signal to the applied driving voltage. The modulated voltage must remain positive and above the turn-on value for the LED to emit light, so the AC signal is often applied with a DC bias. Such an approach allows complex modulation schemes to be employed in the AC signal, such as pulse amplitude modulation (PAM) and orthogonal frequency division multiplexing (OFDM), and is often used for high data rate, single transmitter demonstrations [4]. However, LED luminosity is non-linearly dependent on the current flow through the active region of a device, so the relationship between the electrical driving signal and the output optical signal is highly non-linear. Fig. 4(a) shows this schematically for a voltage signal. This can have significant impact on complex modulation schemes as the signal becomes distorted, and care must be taken to operate in the quasi-linear region of the luminosity - voltage (L-V), or luminosity - current curve (L-I), restricting the dynamic range of an OWC system.

DC biased AC signals work well for single micro-LED transmitters, as the emitter can be wire-bonded to a printed circuit board (PCB) where arbitrary electrical signals can be applied by a suitable external driver, typically an arbitrary wave-form generator (AWG) or a digital to analogue converter (DAC). This approach can yield high data rates with low-density arrays

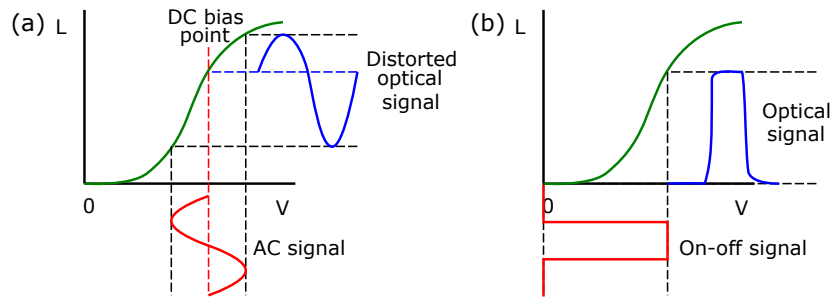


**Figure 4.** Schematics of (a) modulation of an LED with a DC biased AC signal. Input electrical signals (red) can be distorted in the optical output (blue) by the nonlinear characteristics of an LED (green). (b) Modulation by on-off switching.

of micro-LEDs [31,32], however, there are obvious scaling problems for the addressing of high density arrays at rates producing Mb/s - Gb/s data signals typically expected of OWC.

Therefore, a common and much simpler approach is full on/off switching of the LED pixels as indicated in Fig. 4(b). This is typically realised through p-type MOS (PMOS) or n-type MOS (NMOS) field effect transistors (FETs) connected to the anode/cathode of the LEDs, and thus readily implemented in high-density active matrix arrays. While NMOS transistors provide higher switching speeds and lower area requirements than PMOS transistors, they need to be connected to the LED cathodes. Standard GaN epitaxial structures have the p-type material on top, due to the low conductivity of p-type GaN, thus imposing significant fabrication challenges when using NMOS drivers, including etching down to the sapphire substrate and depositing several insulation layers [33]. Therefore, NMOS drivers are only used in a few select cases where fast switching speeds were desired, and PMOS drivers are much more commonly used.

Using such on/off switching, micro-LED pixels can also (when required) be driven by extremely short electrical pulses, with frequency components beyond the modulation bandwidth of the device. This has produced optical pulses as short as 300 ps with an output power density of  $\approx 10 \text{ W cm}^{-2}$  [16].

### (b) Highly-parallel digital electronic interfacing

As discussed above in section 3(a), micro-LED based OWC systems will in practice rely on driving through either DACs or FETs, both of which can be directly controlled through digital electronic signals. These digital control signals in turn are supplied through application specific integrated circuits (ASICs), micro-controllers, or through field-programmable gate arrays (FPGAs). All of these provide a low footprint in terms of size, weight and power (SWaP), thus retaining this important property of micro-LEDs, and they can connect to standard computer interfaces such as universal serial bus (USB).

Micro-controllers are convenient and sometimes used for proof-of-principle demonstrations, but their performance does not match the capabilities of micro-LED systems. ASICs are very powerful, but their development is time-consuming and costly, so they are only used in research if there is no simpler method to achieve the operating target. FPGAs are more difficult to use than micro-controllers, but they offer comparable performance to ASICs and allow exact control of latencies. Consequently, FPGAs have become increasingly important for digitally interfaced experiments and underpin many of the applications discussed below in sections 4 and 5.

The integrated nature of a micro-LED array bonded to bespoke CMOS control electronics, combined with digital control through FPGA devices, provides a compact optical transmitter system capable of high speed spatial and temporal modulation of optical signals. An optimised system could be developed on the scale of a few  $\text{cm}^2$ , with a power consumption of less than 1 W and very low mass on the order of a few 100's of grams [34]. This allows the multi-functional OWC

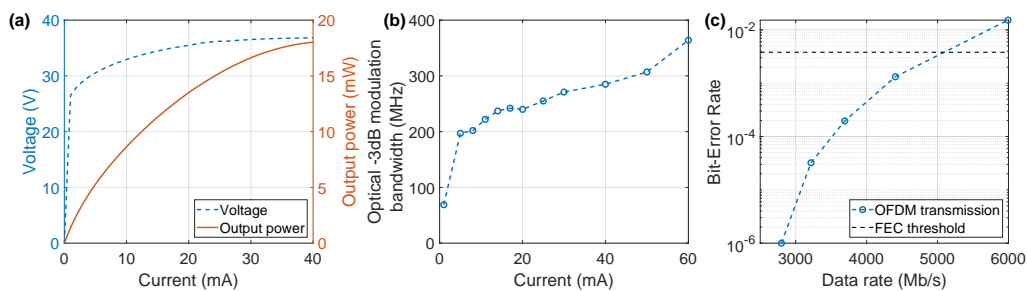


**Figure 5.** (a) Electro-optical performance of 9 micro-LEDs connected in series. (b) Modulation bandwidth and (c) data rate performance using OFDM [18].

systems described in this paper to be implemented in application areas with SWaP limitations, such as small satellites, drones, internet-of-things devices, and wearable technology.

## 4. Micro-LED enabled OWC

As the bottleneck for OWC systems is often the optical transmitter, the high modulation bandwidth exhibited by micro-LEDs enables high data rate transmission. A detailed discussion of modulation schemes, multiplexing techniques, and hardware that underpin Gb/s OWC is given by Rajbhandari *et al.* [4], which provides an extensive review of visible light communications using GaN devices, including micro-LEDs, up to 2016. It is worth noting, however, that since its publication single micro-LED pixels using OFDM have reached data rates of almost 10 Gb/s [35]. The OWC results discussed in this paper will instead focus on communications demonstrations that take explicit advantage of the micro-LED format, regardless of the achieved data rates.

### (a) Series-connected micro-LED transmitters

The high modulation bandwidth nature of a micro-LED is an advantage for high data rate transmission, however, the reduced size also reduces total output power. In turn, this reduces the achievable signal-to-noise ratio at a receiver, which can limit the performance of an optical link. This is of particular importance for application areas where high levels of loss may be experienced in the optical channel, such as for underwater optical wireless communications (UOWC), where light is scattered and absorbed in water [36]. An obvious approach to increase transmitter power, particularly in arrayed devices, is to increase the number of pixels in use. However, to preserve the modulation bandwidth of single micro-LEDs operated in parallel, each pixel must have an individual set of drive electronics, which becomes impractical for complex modulation schemes, as discussed in Section (a).

An alternative approach is to connect the pixels in series, as shown schematically in Fig. 1(e) [18]. By fully isolating micro-LED mesas down to the sapphire substrate, metal tracks can be deposited to interconnect LEDs from cathode to anode. Fig. 5(a) shows the electro-optical performance of a series device composed of 9 circular, 40  $\mu\text{m}$  diameter micro-LEDs. Naturally, the turn-on voltage for the device is increased by a factor of 9 over that of a single pixel due to the series connection. The device is able to produce 18 mW of optical power before thermal rollover, slightly less than 9 times that of a single pixel due to heating effects and light absorption by neighbouring pixels. Importantly, Fig. 5(b) shows that the high modulation bandwidths are preserved, achieving over 280 MHz at 3200  $\text{A cm}^{-2}$ .

Achievable data rates were investigated when using the 9-element series device for free space optical communications. Fig. 5(c) shows the bit-error-ratio (BER) against data rate performance using OFDM. A BER below a forward error correction (FEC) threshold, indicated in Fig. 5(c), can be considered “error free” with application of an FEC algorithm. The BER curve intersects the FEC

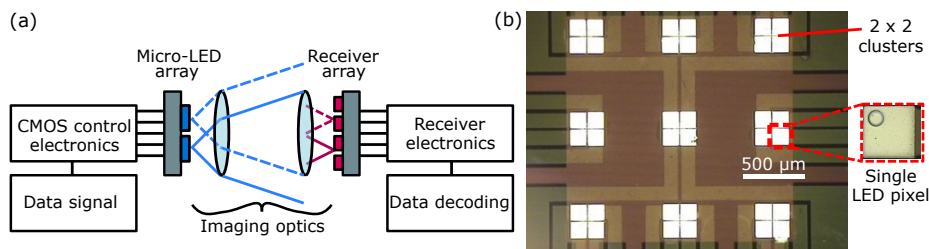


**Figure 6.** (a) Schematic of an imaging MIMO setup. (b) Plan view optical micrograph of a micro-LED array for MIMO with a  $3 \times 3$  set of  $2 \times 2$  clusters of  $39 \mu\text{m}$  LED pixels.

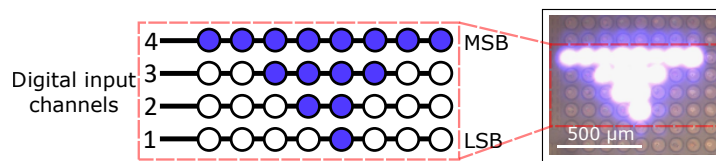


**Figure 7.** Schematic and plan view optical micrograph of a section from a  $16 \times 16$  CMOS controlled micro-LED array with binary weighted groups of pixels enabled. Applying digital signals to each column can produce  $2^4$  discrete signals.

threshold at a data rate of 5.18 Gb/s. Therefore, as the FEC algorithm introduces a 7% overhead, the error free data rate achieved with the series device is 4.81 Gb/s.

## (b) MIMO transmitters

The performance of 4G and 5G RF mobile wireless networks is crucially underpinned by employing MIMO techniques to multiplex data over arrays of transmitters and de-multiplex them using an array of receivers. While the de-multiplexing of MIMO channels is generally a matrix inversion on the vector of received signals, adaptation to OWC enables an enhanced approach called “imaging MIMO”. In this case, optics at both transmitter and receiver arrays aid the channel separation process by physically separating the signals incident on the receiver array as indicated in Fig. 6. Micro-LEDs are ideally suited for this application, not only for their high bandwidth, but also because they can be fabricated into a low density array of emitters that are spaced sufficiently apart on the one hand to allow efficient optical channel separation, yet on the other hand are sufficiently close to each other to remain in the field of view of standard lens optics. Up to 7 Gb/s were demonstrated using a  $3 \times 3$  array of LEDs using one  $39 \mu\text{m}$  diameter pixel from each cluster of the device shown in Fig. 6(b) [32,37].

## (c) Digital to light conversion

In Section 3 the non-linearity issues arising from the use of a single LED transmitter were highlighted, which may be exacerbated by non-linearities of the DAC. This can seriously distort the transmitted waveforms and result in bit errors. However, with an LED array, discrete levels can be generated by activating binary weighted groups of LEDs. With a CMOS-controlled micro-LED array, as in Fig. 7, this functionality is available on a mm-sized chip with digital control [38]. In effect, digital signals are directly converted to optical, removing the need for a DAC and avoiding the non-linearity issues of a single pixel.

This approach has been used to demonstrate 4 and 8 level PAM with a symbol rate of 100 MHz [39]. In addition, analogue signals can be quantised into discrete levels, allowing the device to output OFDM signals despite being limited to on-off modulation of each pixel. This demonstrated



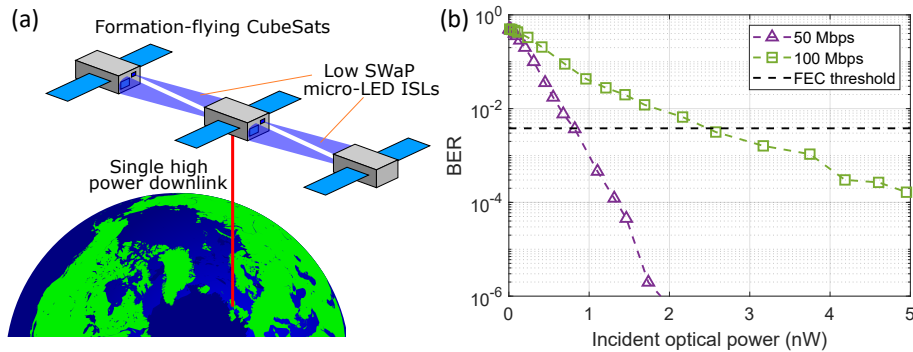


**Figure 8.** (a) Intersatellite links (ISLs) between formation flying CubeSats are provided by low SWaP micro-LED hardware. (b) Transmission results indicating low received optical power levels.

a spectral efficiency of 3.96 bits/s/Hz, though the data rate was limited by the maximum 100 MHz sampling rate of the FPGA [39].

#### (d) Low SWaP photon-counting communications

An important property of micro-LEDs is their small footprint, which even when combined with driver electronics can remain on a chip-scale level, with power consumption at or below the 1 W level. This makes them attractive for systems on mobile platforms, robots, underwater-vehicles, drones, or nano-satellites. Many of these applications come with significant link distances, and the low overall optical output powers of micro-LEDs then require suitably sensitive detectors. This demand can be met by single photon avalanche diodes (SPADs) [40], which combine photon-level sensitivity with a time resolution on the order of 100 ps. These devices offer low footprint, digital electronic interfacing, and spectral sensitivity which matches well with micro-LED emission.

Demonstrations using just a single micro-LED transmitter and SPAD-based receivers indicated that data rates of up to 100 Mb/s can be achieved with very low received power levels, while meeting the power constraints of typical nano-satellite platforms [34,41]. A potential application scenario is shown in Fig. 8(a), where a network of CubeSats could communicate with low SWaP micro-LED systems, with only one unit requiring a higher power downlink system. Fig. 8(b) shows the required received power levels are low, and ray-tracing simulations indicate these levels can be maintained over multi-km ranges with simple optics [42].

## 5. Structured light capabilities linking imaging, tracking, and communications

Driven initially by the prospect of high-brightness micro-displays, GaN micro-LEDs have been fabricated into high density arrays with active-matrix control. The prospect of utilising this high degree of spatial diversity for OWC was exploited soon after creation of these devices, and preliminary results by indicated that Gb/s rates should be attainable [43]. Since then, there have been technology demonstrations highlighting an array of novel capabilities of active-matrix micro-displays. In this section, we provide a review of the early activities in this emerging field.

#### (a) Mobile phone camera communications through spatial patterns

Optical camera communications (OCC) is an attractive method for data transfer due to the widespread availability of high resolution camera systems in portable consumer products, such as smartphones and laptops [44]. Although any device with an image sensor could receive an

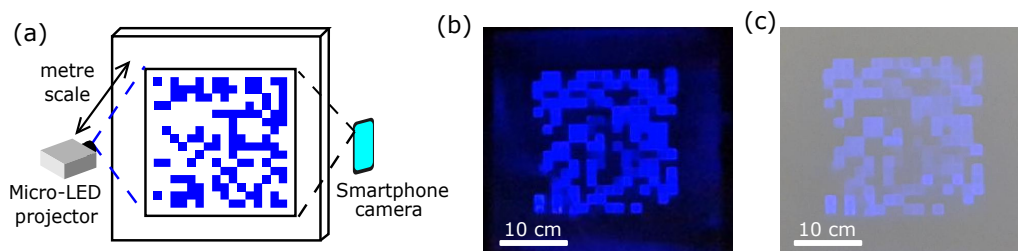


**Figure 9.** (a) Schematic of the OCC system using a micro-LED projector and smartphone camera. Example pseudorandom frames displayed on a wall under (b) dark conditions and (c) normal room lighting.

OWC signal, a common problem is the frame rate of the camera, typically 30 or 60 fps, which strongly limits the sampling rate of a signal and therefore data rate. However, smartphones are increasingly being produced with slow motion camera systems with frame rates up to 240 fps, and some up to 960 fps. This can lift some of the data rate ceilings of OCC methods, though for maximum performance it is important for the system to fully exploit both spatial and temporal domains as much as possible.

A micro-LED array with suitable optics can be operated as a projector system, displaying structured light patterns on a surface [45]. With this approach, shown schematically in Fig. 9(a), OWC can be achieved through the patterns imaged by a smartphone camera. Each pixel in the micro-LED array transmits an independent on-off keying (OOK) data stream, resulting in patterns that appear pseudorandom, as shown in Figs. 9(b) and (c). Data rates can be scaled in the spatial domain, by adding pixels and therefore parallel streams, or temporal domain, by increasing the frame rates of the camera and projector. Proof-of-concept experiments have shown a data rate of 122.88 kb/s with a  $16 \times 16$  array of micro-LEDs and a Samsung Galaxy S9 smartphone [45].

The high-speed nature of micro-LED display systems allows the transmitter in this OCC implementation to readily keep pace with the frame rates emerging in consumer camera technology. With a moderate increase in transmitter resolution, data rates scale to Mb/s rates. For example, using the same resolution as a version 19 QR code ( $93 \times 93$ ), a data rate of 4.15 Mb/s could be achieved. In contrast, applying the high frame rate camera to alternative transmitters for spatially encoded OCC results in limited scaling due to transmitter frame rate limitations, whereas the micro-LED systems are limited by the receiver frame rates.

## (b) Data through display

Li-Fi technology relies on the dual use of LEDs for lighting and OWC at the same time. Similarly, micro-LED displays could be made to display content to human users while at the same time transmitting data through an OWC signal that can be sensed by a photodetector. In a first instance, the display could encode the data in frames that are displayed at the standard video frame rate (e.g. 30 fps). This approach was indeed used for high data rate camera communications [46], however, during the data transfer the normal display function is disabled or compromised. The display function would be retained if the display was operated at a high frame rate (kfps or more) and data encoded such that within visually recognisable timescales (about 50 ms) the value of each pixel averages to the grey scale value of the currently displayed image. It would be challenging to do this through individual pixel addressing due to the high data rates required, however, simpler alternatives are possible. A global or row-wise OWC data signal can be overlaid at pixel level with the greyscale setting, such that the correct grey level of the pixel is preserved and the OWC signal is transmitted at a speed invisible to the eye. Li *et al.* [23,47] implemented such a configuration by overlaying PWM for brightness control at 135 fps with a global Manchester-encoded OOK OWC signal at 2 Mb/s, as illustrated in Fig. 10. This approach has since been applied to OCC at a peak rate of 16.6 kb/s and an average rate of 5 kb/s [48].

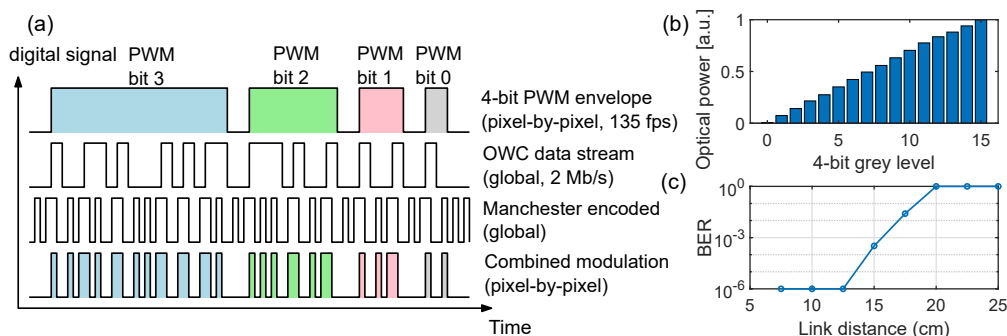


**Figure 10.** Data through display: (a) Modulation scheme with pixel-wise greyscale video display using PWM, overlaid with a global OWC data signal using Manchester-encoded OOK. (b) Normalised optical power of one pixel for 16 levels, data from [23]. (c) BER as a function of distance for 2 Mb/s, simultaneously displaying a video at 135 fps, data from [47].

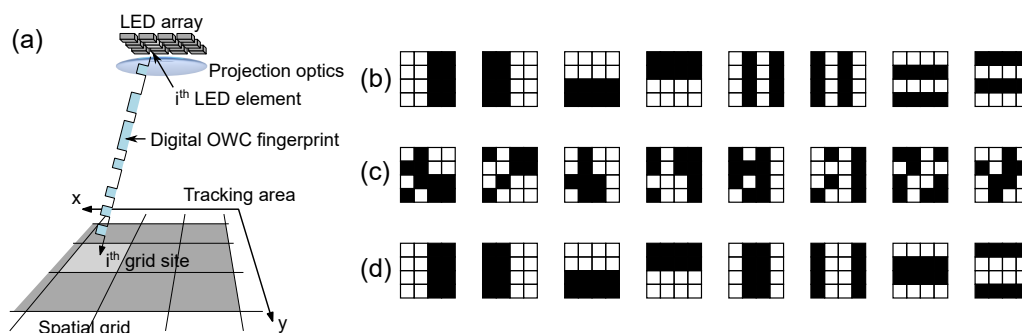


**Figure 11.** (a) Schematic of positioning using digital fingerprints by structured illumination from a micro-LED array. Example pattern sequences for fingerprinting with a  $4 \times 4$  array using (b) binary search, (c) pseudorandom and (d) moving bars patterns.

### (c) Visible light positioning through structured illumination

An active area of research related to OWC is in positioning systems. While the Global Positioning System (GPS) is the dominant technology for self-location across the globe, it has drawbacks in indoor environments, and areas where line-of-sight to the satellites may be blocked. Instead, optical signals from light fittings can be used as local navigation systems, providing high positioning accuracy, and brings similar advantages to optical communications such as no RF interference and integration with solid state lighting [49]. In addition, positioning functionality can be employed in parallel with communication functions, enhancing communication performance by enabling space-division multiple access data transmission and assisting handover between transmitters, important functions for Li-Fi style systems [3,50].

There are many approaches to visible light positioning (VLP), including triangulation, time-of-arrival and probabilistic methods. Structured illumination provided by micro-LED arrays can be used to determine position based on fingerprint signals supplied to a spatial grid [50,51]. The concept is shown schematically in Fig. 11(a), where a micro-LED array is imaged onto a tracking area, with each pixel illuminating a spatially separated area. By careful choice of binary illumination patterns, each area receives a unique set of on-off signals, from which position can be determined. There are many potential binary pattern sequences, with binary search patterns, pseudorandom patterns and “moving bars” patterns shown in Figs. 11(b), (c) and (d) respectively, for an example  $4 \times 4$  array. Larger arrays require more patterns to generate unique signals for

each pixel. The advantages of this approach are low computational complexity, low receiver hardware requirements, and scalability through appropriate optics. Indeed, scaling down to a microscopic level for integration into a direct-writing optical lithography tool has recently been shown [52], and scaling to kilometre link distances is believed to be possible with a suitably sensitive receiver [41]. Flicker-free operation is guaranteed by update rates of up to 30 kfps [53].

## 6. Conclusions and prospects

Micro-LED arrays provide a high-bandwidth technology for many forms of OWC with sophisticated control of the spatial characteristics of the transmitted signal. They are able to meet tight SWaP constraints and can be conveniently interfaced with digital electronics, providing source technology for the emerging application area of structured lighting, which combines high density spatial encoding with the LEDs' fast switching characteristics. Micro-LEDs are well-matched with SPAD receivers, which also offer low SWaP and digital electronic interfacing. Exploiting photon-sensitive detection, micro-LEDs can be used for OWC in challenging environments, e.g. underwater or in space. With ongoing developments of hardware and electronic driving schemes, micro-LEDs are capable contenders for many internet-of-things related applications and are well-placed to foster emerging convergences between lighting, display and communications.

**Data Accessibility.** As this is a review article, there is no associated dataset.

**Authors' Contributions.** MDD, JH and ADG defined the scope of the article, ADG, JH and JJDMcK drafted the manuscript. All authors contributed to its final form and editing.

**Competing Interests.** The authors declare that they have no competing interests.

**Funding.** The authors acknowledge EPSRC for funding. (EP/K00042X/1, EP/M01326X/1, EP/S001751/1)

**Acknowledgements.** The authors acknowledge Robert Henderson (University of Edinburgh) for CMOS support.

## References

1. Kavehrad M. 2013 Optical wireless applications: a solution to ease the wireless airwaves spectrum crunch. *Proc. of SPIE* **8645**. doi:10.1117/12.2001522
2. Karunatilaka D, Zafar F, Kalavally V, Parthiban R. 2015 LED based indoor visible light communications: State of the art. *IEEE Commun. Surveys Tuts.* **17**, 1649–1678. doi:10.1109/COMST.2015.2417576
3. Haas H, Yin L, Wang Y, Chen C. 2015 What is LiFi? *Journal of Lightwave Technology* **34**, 1533–1544. doi:10.1109/JLT.2015.2510021
4. Rajbhandari S, Mckendry JJD, Herrnsdorf J, Chun H, Faulkner G, Haas H, Watson IM, O'Brien D, Dawson MD. 2017 A review of Gallium Nitride LEDs for multi-gigabit-per-second visible light data communications. *Semicond. Sci. Technol.* **32**, 1–44. doi:10.1088/1361-6641/32/2/023001
5. Krames MR, Shchekin OB, Mueller-Mach R, Mueller GO, Zhou L, Harbers G, Craford MG. 2007 Status and Future of High-Power Light-Emitting Diodes for Solid-State Lighting. *J. Display Technol.* **3**, 160–175. doi:10.1109/JDT.2007.895339
6. Barlow IA, Kreouzis T, Lidzey DG. 2009 High-speed electroluminescence modulation of a conjugated-polymer light emitting diode. *Appl. Phys. Lett.* **94**, 243301. doi:10.1063/1.3147208
7. Shen H, *et al.* 2019 Visible quantum dot light-emitting diodes with simultaneous high brightness and efficiency. *Nat. Photonics* **13**, 192–197. doi:10.1038/s41566-019-0364-z
8. Zhang L, *et al.* 2017 Ultra-bright and highly efficient inorganic based perovskite light-emitting diodes. *Nature Communications* **8**, 15640. doi:10.1038/ncomms15640
9. Chun H, Gomez A, Quintana C, Zhang W, Faulkner G, O'Brien D. 2019 A Wide-Area Coverage 35 Gb/s Visible Light Communications Link for Indoor Wireless Applications. *Sci Rep.* **9**, 4952. doi:10.1038/s41598-019-41397-6
10. Humphreys CJ. 2008 Solid-State Lighting. *MRS Bulletin* **33**, 459–470. doi:10.1557/mrs2008.91
11. Day J, Li J, Lie DY, Bradford C, Lin JY, Jiang HX. 2011 III-Nitride full-scale high-resolution microdisplays. *Appl. Phys. Lett.* **99**, 1–4. doi:10.1063/1.3615679

12. Herrnsdorf J, *et al.* 2015 Active-matrix GaN micro light-emitting diode display with unprecedented brightness. *IEEE Trans. Electron Devices* **62**, 1918–1925. doi:10.1109/TED.2015.2416915
13. Guilhabert B, Elfström D, Kuehne AJC, Massoubre D, Zhang HX, Jin SR, Mackintosh AR, Gu E, Pethrick RA, Dawson MD. 2008 Integration by self-aligned writing of nanocrystal/epoxy composites on InGaN micropixelated light-emitting diodes. *Opt. Express* **16**, 18933–18941. doi:10.1364/oe.16.018933
14. Schubert E. 2006 *Light emitting diodes*. Cambridge: Cambridge University Press.
15. Watson IM. 2013 Metal organic vapour phase epitaxy of AlN, GaN, InN and their alloys: A key chemical technology for advanced device applications. *Coordination Chemistry Reviews* **257**, 2120 – 2141. doi:https://doi.org/10.1016/j.ccr.2012.10.020
16. McKendry JJD, Rae BR, Gong Z, Muir KR, Guilhabert B, Massoubre D, Gu E, Renshaw D, Dawson MD, Henderson RK. 2009 Individually addressable AlInGaN micro-LED arrays with CMOS control and subnanosecond output pulses. *IEEE Photon. Technol. Lett.* **21**, 811–813. doi:10.1109/LPT.2009.2019114
17. Liu ZJ, Wong KM, Keung CW, Tang CW, Lau KM. 2009 Monolithic LED Microdisplay on Active Matrix Substrate Using Flip-Chip Technology. *J. Sel. Topics Quantum Electron.* **15**, 1298–1302. doi:10.1109/JSTQE.2009.2015675
18. Xie E, McKendry JJD, Gu E, Dawson MD, Islim MS, He X, Haas H, Purwita A. 2018 High-speed visible light communication based on a III-nitride series-biased micro-LED array. *J. Lightw. Technol.* **37**, 1180–1186. doi:10.1109/jlt.2018.2889380
19. Xu ZH, Chen W, Penuelas J, Padgett M, Sun MJ. 2018 1000 fps computational ghost imaging using LED-based structured illumination. *Opt. Express* **26**, 2427–2434. doi:10.1364/OE.26.002427
20. Choi HW, Jeon CW, Dawson MD. 2004 High-Resolution 128×96 Nitride Microdisplay. *IEEE Electron. Dev. Lett.* **25**, 277–279. doi:10.1109/LED.2004.826541
21. Jeon CW, Kim KS, Dawson MD. 2002 Fabrication of Two-Dimensional InGaN-Based Micro-LED Arrays. *Phys. Stat. Solid. A* **192**, 325–328.
22. Lee YJ, Yang ZP, Chen PG, Hsieh YA, Yao YC, Liao MH, Lee MH, Wang MT, Hwang JM. 2014 Monolithic integration of GaN-based light-emitting diodes and metal-oxide-semiconductor field-effect transistors. *Opt. Express* **22**, A1589–A1595. doi:10.1063/1.96555
23. Li X, Wu L, Liu Z, Hussain B, Chong WC, Lau KM, Yue CP. 2016 Design and characterization of active matrix LED microdisplays with embedded visible light communication transmitter. *J. Lightw. Technol.* **34**, 3449–3457. doi:10.1109/JLT.2016.2562667
24. Jalajakumari AVN, Tsonev D, Cameron K, Haas H, Henderson R. 2015 An energy efficient high-speed digital led driver for visible light communications. *2015 IEEE International Conference on Communications ICC* pp. 5054–5059. doi:10.1109/ICC.2015.7249125
25. Carreira JFC, Guilhabert BJE, McKendry JJD, Xie E, Mathieson K, Watson IM, Gu E, Dawson MD, Henderson RK. 2018 Integration of Micro-LED Array on CMOS by Transfer Printing. *2018 IEEE Photonics Conference* pp. 1–2. doi:10.1109/IPCon.2018.8527266
26. McKendry JJD, Massoubre D, Zhang S, Rae BR, Green RP, Gu E, Henderson RK, Kelly AE, Dawson MD. 2012 Visible-Light Communications Using a CMOS-Controlled Micro-Light-Emitting-Diode Array. *J. Lightw. Technol.* **30**, 61–67. doi:10.1109/JLT.2011.2175090
27. Yang W, *et al.* 2014 Size-dependent capacitance study on InGaN-based micro-light-emitting diodes. *J. Appl. Phys.* **116**, 044512. doi:10.1063/1.4891233
28. Piprek J. 2010 Efficiency droop in nitride-based light-emitting diodes. *Phys. Status Solidi A* **207**, 2217–2225. doi:10.1002/pssa.201026149
29. Green RP, McKendry JJD, Massoubre D, Gu E, Dawson MD, Kelly AE. 2013 Modulation bandwidth studies of recombination processes in blue and green InGaN quantum well micro-light-emitting diodes. *Appl. Phys. Lett.* **102**, 091103. doi:10.1063/1.4794078
30. Tian P, McKendry JJD, Herrnsdorf J, Watson S, Ferreira R, Watson IM, Gu E, Kelly AE, Dawson MD. 2014 Temperature-dependent efficiency droop of blue InGaN micro-light emitting diodes. *Appl. Phys. Lett.* **105**, 171107. doi:10.1063/1.4900865
31. Ferreira R, Xie E, McKendry J, Rajbhandari S. 2016 High bandwidth GaN-based micro-LEDs for multi-Gbps visible light communications. *IEEE Photon. Technol. Lett.* **28**, 1. doi:10.1109/LPT.2016.2581318
32. Rajbhandari S, *et al.* 2017 A multigigabit per second integrated multiple-input multiple-output VLC demonstrator. *J. Lightw. Technol.* **35**, 4358–4365. doi:10.1109/JLT.2017.2694486

33. Xie E, *et al.* 2017 Design, fabrication and application of GaN-based micro-LED arrays with individual addressing by N-electrodes. *IEEE Photon. J.* **9**. doi:10.1109/JPHOT.2017.2768478
34. Griffiths AD, Herrnsdorf J, Almer O, Henderson RK, Strain MJ, Dawson MD. 2019 High-sensitivity free space optical communications using low size, weight and power hardware. *ArXiv e-prints*. <http://arxiv.org/abs/1902.00495>
35. Islim MS, *et al.* 2017 Towards 10 Gb/s orthogonal frequency division multiplexing-based visible light communication using a GaN violet micro-LED. *Photonics Research* **5**, A35–A43. doi:10.1364/prj.5.000a35
36. Kaushal H, Kaddoum G. 2016 Underwater optical wireless communication. *IEEE Access* **4**, 1518–1547. doi:10.1117/1.3280288
37. Rajbhandari S, Chun H, Faulkner G, Haas H, Xie E, McKendry JJD, Herrnsdorf J, Gu E, Dawson MD, O'Brien D. 2019 Neural Network-Based Joint Spatial and Temporal Equalization for MIMO-VLC System. *IEEE Photon. Technol. Lett.* **31**, 821–824. doi:10.1109/LPT.2019.2909139
38. Herrnsdorf J, McKendry JJD, Ferreira R, Henderson R, Videv S, Watson S, Haas H, Kelly AE, Gu E, Dawson MD. 2015 Single-chip discrete multitone generation. *2015 IEEE Summer Topicals Meeting Series, SUM 2015* **2**, 47–48. doi:10.1109/PHOSST.2015.7248185
39. Griffiths AD, Islim MS, Herrnsdorf J, McKendry JJD, Henderson R, Haas H, Gu E. 2017 CMOS-integrated GaN LED array for discrete power level stepping in visible light communications. *Opt. Express* **25**, A338 – A345. doi:10.1364/OE.25.00A338
40. Cova S, Ghioni M, Lacaita A, Samori C, Zappa F. 1996 Avalanche photodiodes and quenching circuits for single-photon detection. *Appl Opt* **35**, 1956. doi:10.1364/AO.35.001956
41. Griffiths AD, Herrnsdorf J, Lowe C, Macdonald M, Henderson R, Strain MJ, Dawson MD. 2018 Temporal encoding to reject background signals in a low complexity, photon counting communication link. *Materials* **11**. doi:10.3390/ma11091671
42. Griffiths AD, Herrnsdorf J, Strain MJ, Dawson MD. 2019 High Sensitivity Inter-Satellite Optical Communications Using LEDs and Single Photon Receivers. *SPACOMM 2019 : The Eleventh International Conference on Advances in Satellite and Space Communications* pp. 36–38.
43. Zhang S, Watson S, McKendry JJD, Massoubre D, Cogman A, Gu E, Henderson RK, Kelly AE, Dawson MD. 2013 1.5 Gbit/s multi-channel visible light communications using CMOS-controlled GaN-based LEDs. *J. Lightw. Technol.* **31**, 1211–1216. doi:10.1109/JLT.2013.2246138
44. Le NT, Hossain MA, Jang YM. 2017 A survey of design and implementation for optical camera communication. *Signal Process-Image* **53**, 95–109. doi:10.1016/j.image.2017.02.001
45. Griffiths AD, Herrnsdorf J, Strain MJ, Dawson MD. 2019 Scalable visible light communications with a micro-LED array projector and high-speed smartphone camera. *Opt. Express* **27**, 15585. doi:10.1364/OE.27.015585
46. Cahyadi WA, Chung YH. 2018 Smartphone camera-based device-to-device communication using neural network-assisted high-density modulation. *Opt. Eng.* **57**, 1–9. doi:10.1117/1.OE.57.9.096102
47. Li X, Cho WK, Hussain B, Kwok HS, Yue CP. 2018 Micro-LED Display with Simultaneous Visible Light Communication Function. *SID Symposium Digest of Technical Papers* **49**, 876–879. doi:10.1002/sdtp.12237
48. Li X, Hussain B, Kang J, Kwok HS, Yue CP. 2019 Smart  $\hat{\text{ij}}$ LED Display-VLC System With a PD-Based/Camera-Based Receiver for NFC Applications. *IEEE Photon. J.* **11**, 1–8. doi:10.1109/JPHOT.2019.2892948
49. Do TH, Yoo M. 2016 An in-Depth Survey of Visible Light Communication Based Positioning Systems. *Sensors* **16**, 678. doi:10.3390/s16050678
50. Herrnsdorf J, Strain M, Gu E, Henderson R, Dawson M. 2017 Positioning and space-division multiple access enabled by structured illumination with light-emitting diodes. *J. Lightw. Technol.* **35**, 2339–2345. doi:10.1109/JLT.2017.2672864
51. Herrnsdorf J, Dawson MD, Strain MJ. 2018 Positioning and data broadcasting using illumination pattern sequences displayed by LED arrays. *IEEE Trans. Commun.* **66**, 5582–5592. doi:10.1109/TCOMM.2018.2850892
52. Stonehouse M, Zhang Y, Guilhabert B, Watson I, Gu E, Herrnsdorf J, Dawson M. 2019 Digital Illumination in Microscale Direct-Writing Photolithography: Challenges and Trade-Offs. *British and Irish Conference on Optics and Photonics, BICOP 2018* pp. 1–4. doi:10.1109/BICOP.2018.8658364
53. Herrnsdorf J, McKendry JJ, Xie E, Strain MJ, Watson IM, Gu E, Dawson MD. 2016 High speed spatial encoding enabled by CMOS-controlled micro-LED arrays. *2016 IEEE Photonics Society Summer Topical Meeting Series, SUM 2016* **2**, 173–174. doi:10.1109/PHOSST.2016.7548774